Transient Extraction Transform Based Fault Location Method with Enhanced Accuracy

Chun Sing Lai*
Brunel Interdisciplinary Power Systems Research Centre, Department of Electronic and Electrical Engineering, Brunel University London, Uxbridge, UB8 3PH United Kingdom
chunsing.lai@brunel.ac.uk

Ning Tong*
Department of Electrical Engineering, School of Automation, Guangdong University of Technology, Guangzhou 510006, China
tongning@gdut.edu.cn

Zhenjie Tang
Department of Electrical Engineering, School of Automation, Guangdong University of Technology, Guangzhou 510006, China
tzj789@qq.com

Ahmed F. Zobaa
Department of Electronic and Electrical Engineering, Brunel University London, Uxbridge, UB8 3PH United Kingdom
azobaa@ieee.org

Zhanlian Li
Department of Electrical Engineering, School of Automation, Guangdong University of Technology, Guangzhou 510006, China
1112104006@mail2.gdut.edu.cn

Loi Lei Lai
Department of Electrical Engineering, School of Automation, Guangdong University of Technology, Guangzhou 510006, China
l.l.lai@gdut.edu.cn

*****Both are the first authors

***Abstract*—The fast determination of internal or external fault for the VSC-MTDC is essential for its safety and continuous operation. As very limited time is permitted in an internal fault, transient-based protection elements are widely applied to locate the fault in a very small-time window. However, with such a short time window, location methods based on the wavelet transform or the mathematical morphology show limited performance balancing the resolution in the time and frequency domains. In recent years, there has been a novel time-frequency domain analysis method, naming the transient extraction transform (TET), with high accuracy in both domains. In this paper, a TET-based fast fault-location method is proposed with enhanced accuracy. Comparison studies are made to highlight the performance of such a method against internal faults for the VSC-MTDC.**

Keywords—fault location, transient extraction transform, VSC-MTDC

I. INTRODUCTION

Voltage source converter-based multiterminal high-voltage direct current (VSC-MTDC) is a promising technique in response to the need for new power systems. With the help of VSC-MTDC, the structure of transmission networks gradually changes from the conventional mode of point-to-point to a stronger one with multiple sending ends and receiving ends, solving the problem of bulk power transmission, large-scale centralized delivery of renewable energy, interconnection of large-scale systems, etc. Compared with the line-commuted converter (LCC) based DC systems, the grid-scale expansion is more convenient for the VSC-MTDC [1]. However, in the case of DC line fault in such a system, the VSC converters are more likely to be blocked due to fault-induced over-current that will damage the electronic switch [2]. Therefore, there is an acute need to accurately identify faults in a very short time window and conduct the fault interruption using a DC circuit breaker (CB). Otherwise, more significant failure may be led to due to the blocking of the VSC converters [3].

At present, many have made generous contributions with various types of countermeasures against DC line fault, especially for single-line grounding fault, since it is the most common one in terms of industrial applications [4]. In literature [5], a fault identification method is proposed based on the ratio of the absolute value of pole-voltage derivatives. As the speed requirement for the protection element is exceptionally high for the VSC-MTDC, say several milliseconds, a very short time window should be used, which affects the selectivity and reliability of the method. In literature [6], A pilot protection scheme based on voltage polarity of the current limiting reactor at the end of the DC line is proposed. Using the local measurement, the requirement for the time-window length could be reduced, thereby increasing the selectivity [7]. In literature [8], the shortfalls of such type of protection element are further discussed in detail. In literature [9], a novel type of local-measurement-based protection element is proposed using the velocity difference of the aerial-modal travelling wave and the zero-modal one. The capture of the arrival of the travelling wave is based on mathematical morphology (MM). Simulation results indicate that using the method above, a very high resistive tolerance could be achieved, and the reach can be as high as approximately 85% of the entire length of the DC line. However, due to the limitation of the MM algorithm in time-domain accuracy, a dead-zone is left at the remote end, as long as the sampling rate is limited in terms of engineering applications.

Recently, the transient extraction transform (TET) has been put forward. It is firstly published in the literature [10] in the field of rotating machinery, where transient signals usually correspond to the failure of the main component, such as a bearing or gear. TET can effectively characterize and extract the transient characteristics of strong frequency modulation signals, especially the pulse-like signals [11]. Based on short-time Fourier transform, TET can effectively characterize and extract transient components from fault signals without the need for extended parameters or a priori information, providing a more concentrated time-frequency representation with an increased feature of the transient component.

The contribution of this paper is to propose a TET-based fault location and protection method for the VSC-MTDC with enhanced accuracy and very limited remote-end dead-zone. Comparison studies are also conducted among TET, the MM, and the wavelet transform, highlighting the perfect performance of the TET applied in the field of high-speed protection elements. In Section II, the basic theory of the TET is introduced. A case is conducted to illustrate the performance of TET in detecting abrupt signals. The methodology of the proposed protection is also given. In Section III, Simulation and

comparison studies are made. Finally, the contributions are concluded in Section IV.

II. Theoretical Studies and Methodology

A. Introduction to TET

To accurately find the arrival time when the aerial-modal travelling wave and zero-modal travelling wave arrive at the local-end protection, based on which the time difference is calculated [9], the TET can be close to the ideal time-frequency analysis (ITFA). That is to say, the time-varying characteristics of travelling wave frequency change can be accurately displayed. The theoretical deduction is as follows [12].

First, a step-function is given by (1):

$$s(t) = A \cdot \delta(t - t_0) \tag{1}$$

STFT is a time-frequency analysis method with good time resolution. The derivation of TET is based on the framework of STFT. The mathematical expression of STFT is as shown in (2):

$$G(t, \omega) = \int_{-\infty}^{+\infty} g(u - t) \cdot s(u) \cdot e^{-i\omega u} du \tag{2}$$

where $g(u\text{-}t)$ is the window function, $s(u)$ is the signal. As the base function of the STFT, $g(u\text{-}t)e^{-i\omega u}$ is moved in the time domain and modulated in the frequency domain to detect any time-varying changes in the signal. To explore the time-frequency energy distribution of STFT results more specifically, (3) can be deduced by substituting (1) into (2):

$$\begin{aligned} G(t, \omega) &= \int_{-\infty}^{+\infty} g(u - t) \cdot A \cdot \delta(t - t_0) \cdot e^{-i\omega u} du \\ &= A \cdot g(u - t_0) \cdot e^{-i\omega t_0} \end{aligned} \tag{3}$$

As $| e^{-i\omega u} | = 1$, therefore, the energy distribution result after STFT of the step-signal can be expressed as (4):

$$|G(t, \omega)| = A \cdot g(u - t_0) \tag{4}$$

The window function g(u) is compact-supported in the time domain. For this reason, the energy distribution of the function $| G(t, \omega) |$ is concentrated in $t=t_0$, and reaches the maximum value of A at this moment. In the time domain, the energy distribution is the largest at t_0, diffuses to the left and right, and the diffusion range is the time support region of the window function $[t_0\text{-}\Delta, t_0\text{+}\Delta]$, where Δ is the time-domain support of the window function. These diffused energy regions will degrade the time resolution, making the step function more challenging to be detected at t_0.

To eliminate the influence of diffusion energy, the time-frequency expression of t_0 is deduced as follows. First, calculate the derivative of $G(t, \omega)$ relative to the frequency variable according to (5):

$$\begin{aligned} \partial_\omega G(t, \omega) &= \partial_\omega \left(A \cdot g(u - t_0) \cdot e^{-i\omega t_0} \right) \\ &= -i t_0 \cdot G(t, \omega) \end{aligned} \tag{5}$$

For any $G(t, \omega) \neq 0$, in the result of STFT, the expression of t_0 relative to the time of t and the frequency of ω can be deduced by (6):

$$t_0(t, \omega) = i \cdot \frac{\partial_\omega G(t, \omega)}{G(t, \omega)} \tag{6}$$

For the STFT of the step signal, the ideal time-frequency analysis result should be that the energy should be concentrated in t_0 rather than diffused in a region. To this aim, it is reasonable to erase the coefficient obtained after excluding the STFT at t_0, and only retain the result of STFT at the moment of step. To achieve this goal, a post-processing process called transient extraction operator (TEO) is proposed, according to (7):

$$TEO(t, \omega) = \delta(t - t_0(t, \omega)) \tag{7}$$

where δ is a step function. When the result of STFT is multiplied by this operator, it means that the values in the neighbourhood of energy diffusion are erased except t_0, as given by (8):

$$Te(t, \omega) = G(t, \omega) \cdot TEO(t, \omega) \tag{8}$$

According to the above analysis, the feature of time-frequency characteristics of step signal under TET can be shown clearly. However, although the travelling wave has the feature of a step function, it is not an ideal step signal for DC line faults. For this reason, there will be some significant problems in terms of practical application. Therefore, it is needed to use the differential of the travelling wave signal.

As $Te(t, \omega)$ is a two-dimensional function of time and frequency, it is needed that such a signal only changes with time so that the arrival of travelling waves can be sensitively captured in the time domain. To this aim, all frequency STFT coefficients are superimposed, and at the same time, the energy distribution is obtained. This process can be described as (9):

$$\left| Te_{\sum} \right|(t) = \left| \sum_{\omega=0}^{\omega_{\max}} Te(t, \omega) \right| \tag{9}$$

For an illustrative purpose, a step function of $\delta(t\text{-}t_0)$ is shown in Fig. 1(a), which is used as a sample of the fault-induced signal at t=5 ms. The sampling rate is set to 200 kHz. To better illustrate TET's superior time-frequency analysis performance, STFT and TET are employed to analyze the step function, where Figs. 1(b) and (d) are respectively from the energy spectrum and STFT frequency domain superposition obtained after STFT. The energy diffuses from 5 ms to the left and good neighbourhoods, and it is not easy to obtain the accurate time of the signal abruption. When using TET, it can be seen from Fig. 1(c) that the capacity distribution can be concentrated at the signal abruption point, the diffusion energy is eliminated, and the interference caused by the energy leakage caused by the so-called 'fence effect' is avoided. In Fig. 1(e), the superposition amount of TET in the frequency domain also rises at the point of 5 ms accurately

In addition, as shown in Figs. 1(d) and (e), Although STFT is similar to TET, all of them can generate a maximum value of frequency domain superposition for a step signal. The signal mutation caused by the arrival of travelling waves is not

an ideal step signal. As a result, the energy diffusion phenomenon will be more severe. It could happen when there is even no maximum value of frequency domain superposition, making it more challenging to obtain the arrival time. However, the capability of the TET is strong enough to eliminate significantly the interference caused by energy diffusion so that it is possible to determine the arrival time of the travelling wave within the allowable level of error.

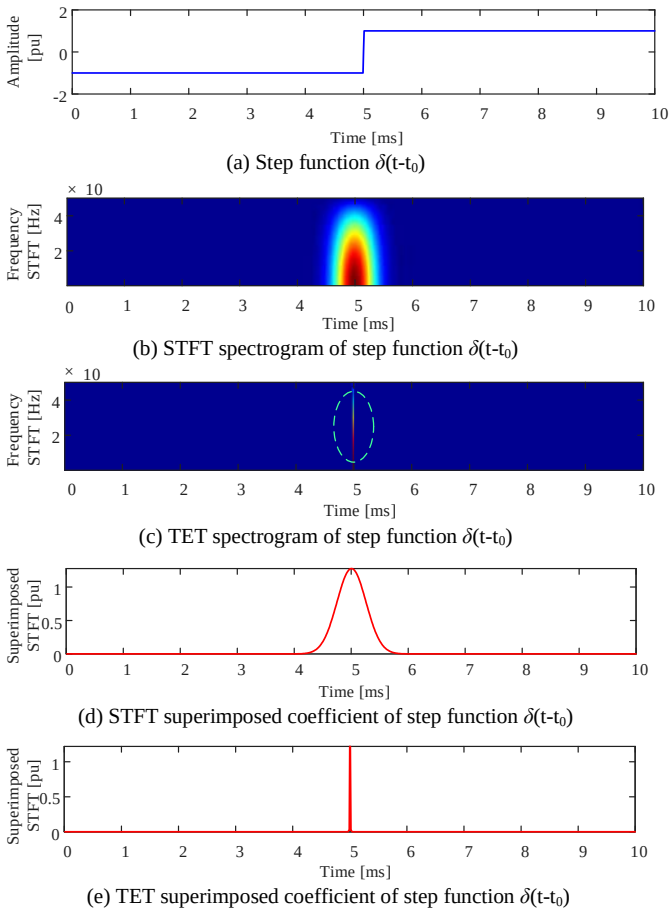

(a) Step function $\delta(t-t_0)$

(b) STFT spectrogram of step function $\delta(t-t_0)$

(c) TET spectrogram of step function $\delta(t-t_0)$

(d) STFT superimposed coefficient of step function $\delta(t-t_0)$

(e) TET superimposed coefficient of step function $\delta(t-t_0)$

Fig. 1. Compared performance between STFT and TET in a step function

B. *The TET-based fault location method*

According to the frequency-dependent characteristics of the DC transmission line, the travelling wave propagation coefficient can be expressed by (10):

$$\gamma_k = \sqrt{\left(\left(G_k(\omega) + \mathrm{j}\omega C_k(\omega)\right)\left(R_k(\omega)\right) + \mathrm{j}\omega L_k(\omega)\right)} \quad (10)$$

where k is the mode symbol for zero-modal (k=0) or aerial-modal (k=1). $G_k(\omega)$, $C_k(\omega)$, $R_k(\omega)$ and $L_k(\omega)$ represent the k-mode conductance, capacitance, resistance, and inductance of the faulted transmission line at frequency ω. (10) can be written in the form of (11):

$$\gamma_k = \alpha_k(\omega) + \mathrm{j}\beta_k(\omega) \quad (11)$$

where $\alpha_k(\omega)$ is the attenuation coefficient and $\beta_k(\omega)$ is the phase-shift coefficient. There are apparent differences in propagation characteristics between aerial-modal and zero-modal travelling waves. When a fault occurs in the DC line, the initial travelling wave is a signal with a broad spectrum. On a long-distance transmission line, due to the influence of reactance and other factors, if the travelling wave passes through a low-pass filter in the propagation process, the high-frequency component of the aerial-/zero-modal travelling wave will be attenuated. For this reason, obvious differences can be observed in the propagation velocity of aerial-/zero-modal travelling waves under lower-frequency components, as shown in Fig. 2.

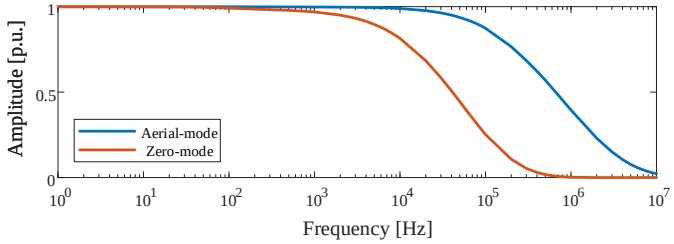

Fig. 2. The characteristic of travelling wave propagation

Based on the above characteristic, the arrival times of aerial-/zero-modal travelling waves can be accurately captured with the TET algorithm. The time difference between them can be captured according to the fault.

C. *Methodology*

The criterion of the main protection can be referred to [9]. This non-unit protection element is based on the arrival time difference (τ=|t_1-t_0|) of aerial and zero-mode travelling waves. The mathematical expression of primary protection can be given by (12):

$$\begin{cases} |t_1 - t_0| < \tau & \text{(1) Internal fault} \\ |t_1 - t_0| > \tau & \text{(2) External fault} \end{cases} \quad (12)$$

As discussed above, the detailed flowchart of the proposed criterion is shown in Fig. 3.

III. Simulations

A 500-kV VSC-MTDC system is established using the PSCAD/EMTDC software, as shown in Fig. 4. First, simulation studies are conducted to identify the arrival time difference when the fault occurs on different Line 12, according to which Table 1 is established. Note that Line 12 is 184.4 km, and part of the faults are external ones. The sampling rate is 200 kHz. As indicated, limited by the sampling rate, the sampling interval is 5 μs.

For this reason, the criterion could not identify the location of the fault when the fault is over 180 km from relay B_{12}. Therefore, τ is set to 0.075 ms, and the reach is 0-180 km (97.6%). Considering the impact of normal operating, starting, and blocking of the system, E_{set} is set to 500 kV^2, and R_{set} is set to 50.

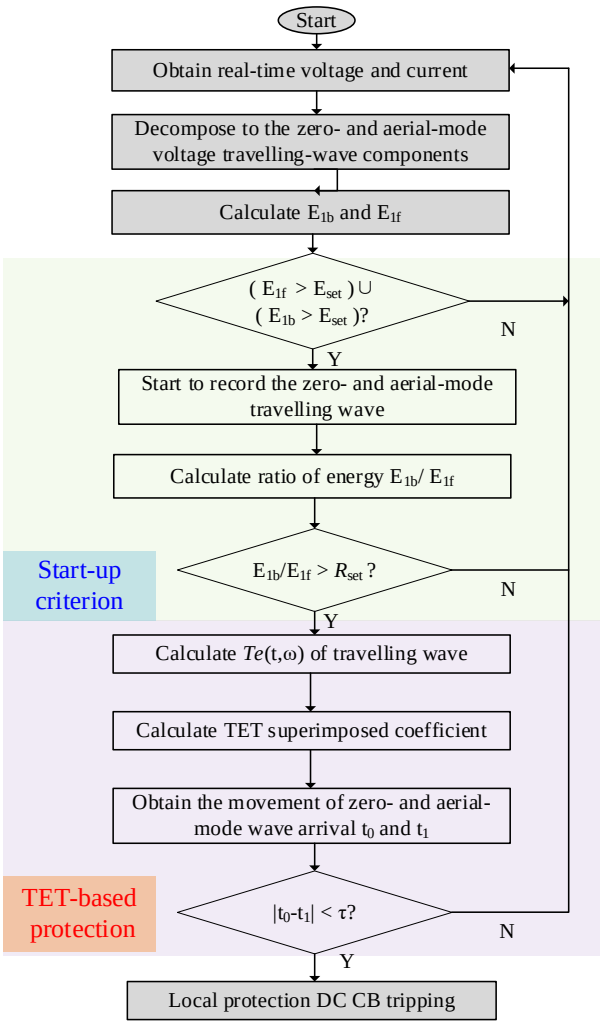

Fig. 3. The flowchart of the proposed criterion

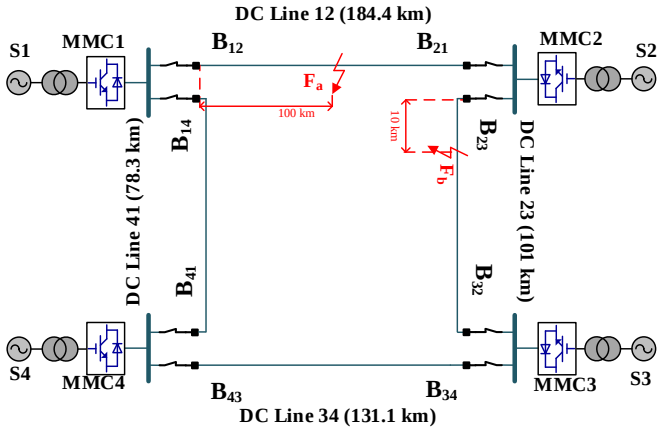

Fig. 4. The topology of the MMC-MTDC system

A. *Internal fault condition*

On DC line 12, a single-line-to-ground fault occurs at F_a, 100 km from the relay B_{12}. Fig. 5(a) shows the variation of the forward traveling wave and the reverse travelling wave. Evidently, in Fig. 5(b), the criterion starts up as the energy ratio criterion is satisfied, indicating a forward fault. In Fig. 5(c), the superimposed coefficient of the TET is shown. Using the TET, it is detected that the arrival time of the aerial-modal wave is t_1, and that of the zero-modal wave is t_0. As $|t_0-t_1|$=0.030 ms<τ, the fault is determined as internal.

TABLE 1. FAULT LOCATION AND TIME DIFFERENCE

Fault location (km)	t_1 *(ms)*	t_0 *(ms)*	τ*(ms)*
100	0.345	0.375	0.030
140	0.478	0.525	0.047
170	0.572	0.642	0.070
180	0.610	0.685	0.075
190	0.648	0.728	0.080
200	0.686	0.771	0.085
210	0.769	0.859	0.090
220	0.852	0.947	0.095
230	0.935	1.035	0.100

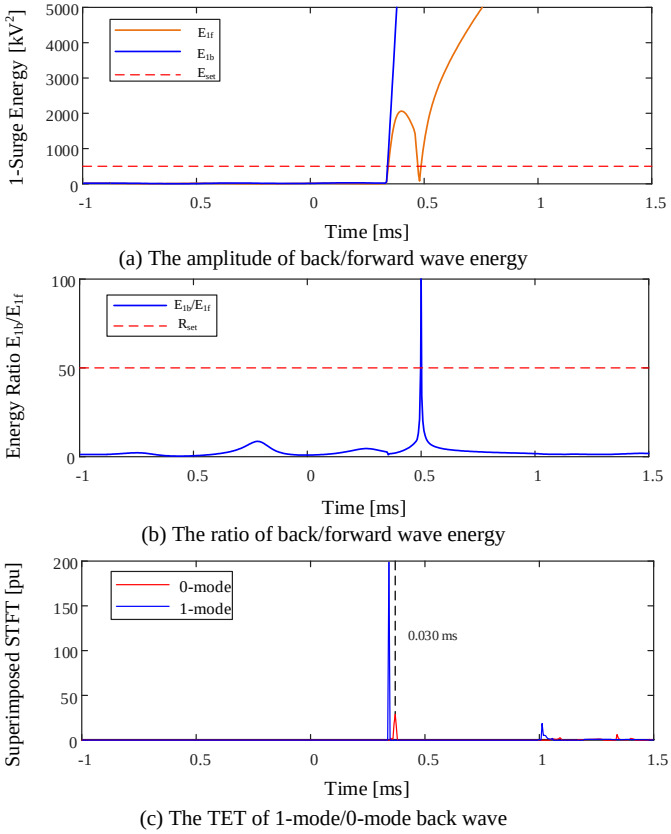

Fig. 5. Energy and time difference criterion under forward internal faults

B. *External fault condition*

On DC line 23, a fault occurs 10 km from the relay B_{23}. For relay B_{12}, this is an external fault. Fig. 6(a) shows the variation of the forward traveling wave and the reverse travelling wave. Evidently, in Fig. 6(b), the criterion starts up as the energy ratio criterion is satisfied, indicating a forward fault. In Fig. 6(c), the superimposed coefficient of the TET is shown. Using the TET, it is detected that the arrival time of the aerial-modal wave is t_1, and that of the zero-modal wave is t_0. As $|t_0-t_1|$=0.090 ms>τ, the fault is determined as external.

C. *Comparison studies*

From the above analysis and tests, it is evident that the reach and accuracy of the main protection are partly determined by the sampling frequency and the algorithm used to detect the arrival time of the travelling wave. The higher the sampling frequency is, the smaller the dead zone will be. For a determined sampling rate, the performance of different algorithms is studied, and the results are shown in Fig. 7. In this paper, conventional algorithms, such as the MM and the wavelet transform, are used to capture the arrival of the

travelling wave under a sampling rate of 200 kHz. According to the results, the reach and the performance of the protection are also highly related to the algorithm we use. For the wavelet transform, the sensitivity should be sacrificed to ensure the protection's selectivity.

For this reason, the reach is merely 70%-80%. By using MM, an enhanced performance could be reached, but the result is not perfect. Using TET, the reach of the main protection can be significantly increased. Over 97% of the entire length of the DC line can be covered, even when the fault resistance is as high as 300 Ω.

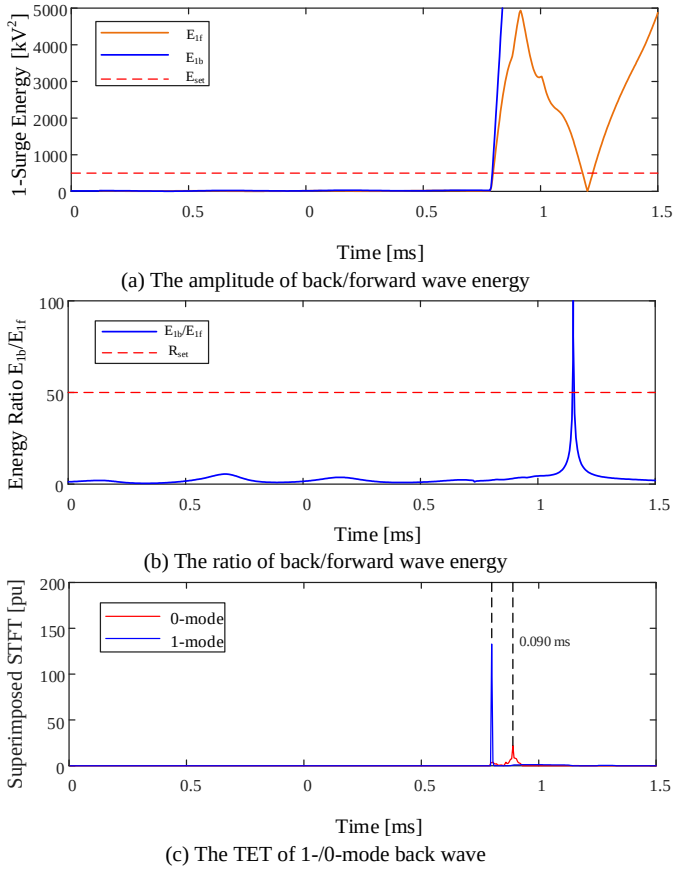

(a) The amplitude of back/forward wave energy

(b) The ratio of back/forward wave energy

(c) The TET of 1-/0-mode back wave

Fig. 6. Energy and time difference criterion under forward external faults

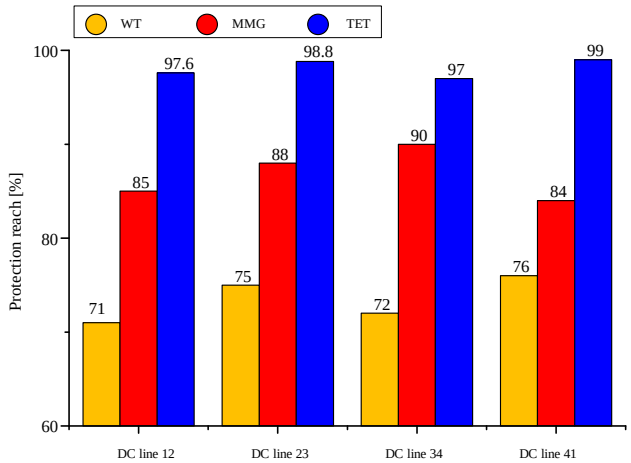

Fig. 7. Comparisons of protection reach with different algorithms

IV. Conclusions

In this paper, a TET-based fast fault location method has been proposed, and simulation results have been used to demonstrate the enhanced accuracy gained. In particular, comparison studies have been used to highlight the better performance of such a new method against internal faults for the VSC-MTDC.

Acknowledgement

This work is supported by the National Natural Science Foundation of China under Grant No. 51907069 and the Natural Science Foundation of Guangdong Province under Grant No. 2021A1515012398.

References

[1] J. Beerten, S. Cole, and R. Belmans, "Generalized steady-state VSC MTDC model for sequential AC/DC power flow algorithms," *IEEE Transactions on Power Systems*, vol. 27, no. 2, pp. 821–829, May 2012.

[2] W. Lu and B. T. Ooi, "DC overvoltage control during loss of converter in multiterminal voltage-source converter-based HVDC (M-VSC-HVDC)," *IEEE Transactions on Power Delivery*, vol. 18, no. 3, pp. 915–920, Jul. 2003.

[3] X. Lin, Y. Zheng, N. Tong, Z. Li, and Q. Sui, "Fast Mutual-Speed-Up Protection Adaptive to Dead-Zone Grounding-Fault Identification for VSC-MTDC," *IEEE Transactions on Power Delivery*, vol. 36, no. 6, pp. 3393–3403, Dec. 2021.

[4] M. Stumpe, P. Ruffing, P. Wagner, and A. Schnettler, "Adaptive Single-Pole Autoreclosing Concept with Advanced DC Fault Current Control for Full-Bridge MMC VSC Systems," *IEEE Transactions on Power Delivery*, vol. 33, no. 1, pp. 321–329, Feb. 2018.

[5] G. Song, Z. Chang, C. Zhang, S. T. H. Kazmi, and W. Zhang, "A High Speed Single-Ended Fault-Detection Method for DC Distribution Line - Part II: Protection Scheme," *IEEE Transactions on Power Delivery*, vol. 35, no. 3, pp. 1257–1266, Jun. 2020.

[6] Q. Huang, G. Zou, S. Zhang, and H. Gao, "A Pilot Protection Scheme of DC Lines for Multiterminal HVDC Grid," *IEEE Transactions on Power Delivery*, vol. 34, no. 5, pp. 1957–1966, Oct. 2019.

[7] C. Li, P. Rakhra, P. Norman, P. Niewczas, G. Burt, and P. Clarkson, "Modulated low fault-energy protection scheme for DC smart grids," *IEEE Transactions on Smart Grid*, vol. 11, no. 1, pp. 84–94, Jan. 2020.

[8] S. D. A. Fletcher, P. J. Norman, S. J. Galloway, P. Crolla, and G. M. Burt, "Optimizing the roles of unit and non-unit protection methods within DC microgrids," *IEEE Transactions on Smart Grid*, vol. 3, no. 4, pp. 2079–2087, 2012.

[9] N. Tong et al. , "Local Measurement-Based Ultra-High-Speed Main Protection for Long Distance VSC-MTDC," *IEEE Transactions on Power Delivery*, vol. 34, no. 1, pp. 353–364, 2019.

[10] G. Yu, "A Concentrated Time-Frequency Analysis Tool for Bearing Fault Diagnosis," *IEEE Transactions on Instrumentation and Measurement*, vol. 69, no. 2, pp. 371–381, 2020.

[11] Z. Li, J. Gao, Z. Wang, N. Liu, and Y. Yang, "Time-Synchroextracting General Chirplet Transform for Seismic Time-Frequency Analysis," *IEEE Transactions on Geoscience and Remote Sensing*, vol. 58, no. 12, pp. 8626–8636, Dec. 2020.

[12] Y. Liu, H. Guo, G. Zhu, and G. Yu, "Single-pole fault protection for MMC-HVDC transmission line based on improved transient-extracting transform," *International Transactions on Electrical Energy Systems*, vol. 31, no. 12, pp. 1–21, 2021.